Origin of Unusually High Rigidity in Selected Helical Coil Structures

David Tománek and Arthur G. Every

Phys. Rev. Applied **8**, 014002 — Published 10 July 2017

DOI: 10.1103/PhysRevApplied.8.014002

Origin of Unusually High Rigidity in Selected Helical Coil Structures

David Tománek[1,*] and Arthur G. Every[2]

[1] *Physics and Astronomy Department, Michigan State University, East Lansing, Michigan 48824, USA*
[2] *School of Physics, University of the Witwatersrand, Private Bag 3, 2050 Johannesburg, South Africa*

(Dated: June 12, 2017)

Using continuum elasticity theory, we describe the elastic behavior of helical coils with an asymmetric double-helix structure and identify conditions, under which they become very rigid. Theoretical insight gained for macro-structures including a stretched telephone cord and an unsupported helical staircase is universal and of interest for the elastic behavior of helical structures on the micro- and nanometer scale.

PACS numbers: 63.22.-m, 62.20.de, 62.25.Jk

I. INTRODUCTION

Helical coil structures, ranging from a stretched telephone cord in Fig. 1(a) and an unsupported spiral staircase in Fig. 1(b) on the macro-scale to DNA and proteins on the micro-scale abound in Nature. Since their elastic behavior is governed by the same laws of Physics independent of scale, insight obtained on the macro-scale will benefit the understanding of helical micro- and nanostructures. An intriguing example of unusual high rigidity on the macro-scale, which has remained unexplained to date, is the unsupported all-wooden spiral staircase in the Loretto Chapel[1] in Santa Fe, New Mexico, constructed around 1878 and shown in Fig. 1(b). In the following we explore the elastic behavior of this structure using continuum elasticity theory in order to identify the reason for its rigidity[2–4]. Since continuum elasticity theory applies from nanometer-sized fullerenes and nanotubes[5–7] to the macro-scale, we expect our approach to be useful to explore the rigidity of helical structures on the micro- and nanometer scale.

The use of continuum elasticity theory rather than the case-specific finite-element method[3] in this case is motivated by our objective to identify the universal origin of the high rigidity of the Loretto spiral staircase and related helical coils with an asymmetric double-helix structure. Theoretical insight gained for macro-structures including a stretched telephone cord and an unsupported helical staircase is universal and of interest for the elastic behavior of helical structures on the micro- and nanometer scale.

II. ELASTIC BEHAVIOR OF A HELICAL COIL

From a Physics viewpoint, the spiral staircase of Fig. 1(b) is a compression coil or a helical spring with a rather high pitch. It can be characterized as an asymmetric double-helix structure consisting of an inner stringer coil of radius R_i and an outer stringer coil of radius R_o, and spans two turns in total. The two stringer coils are connected by rigid steps of width $R_o - R_i$. The staircase

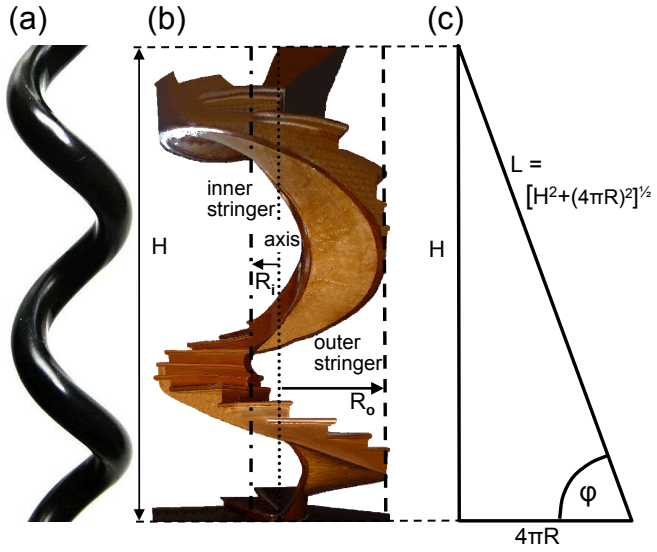

FIG. 1. (a) Photograph of a coiled telephone cord with the same topology as an unsupported spiral staircase. (b) Retouched photograph of the unsupported spiral staircase at the Loretto Chapel as constructed. (c) Trace of the helical inner or outer stringers of the staircase on the surface of a cylinder, which can be unwrapped into a rectangle.

can be equivalently described as a helicoid, or a "filled-in" helix, with finite nonzero inner and outer radii.

There is an extensive literature on the properties of helical springs, which dates back to Love's treatise[2], as well as the more recent Refs. [3,4] and literature cited therein. Yet the compound helical structure of the Loretto staircase and related helical coils appears to have escaped attention in publications so far. The rigidity of the connecting steps provides the spiral staircase with a remarkable degree of stiffness, as we show below. We propose that this property is shared by similar helical structures independent of their scale.

Any coil of radius R and total height H, such as the inner and the outer stringer of the staircase, lies within a cylindrical wall of the same height, which can be unwrapped onto a triangle, as shown in Fig. 1(c). Let us

first consider the case of incompressible inner and outer stringers of height H that are separated by the constant distance $R_o - R_i$, which defines the step width.

According to Fig. 1(c), the equilibrium length L_i of the inner stringer coil with two turns is related to its equilibrium radius R_i and its equilibrium height H by

$$L_i^2 = H^2 + (4\pi)^2 R_i^2 \,. \tag{1}$$

The equivalent relation applies, of course, to the outer stringer of radius R_o.

We first consider an incompressible stringer of constant length L_i, which is stretched axially by δH, causing the radius R_i to change by δR_i. Then,

$$L_i^2 = (H + \delta H)^2 + 16\pi^2 (R_i + \delta R_i)^2 \,. \tag{2}$$

Subtracting Eq. (1) from Eq. (2) and ignoring δH^2 and δR_i^2 terms in the limit of small deformations, we obtain

$$2H\delta H + 16\pi^2 (2R_i \delta R_i) = 0 \tag{3}$$

and consequently

$$\delta R_i = -\frac{H}{16\pi^2 R_i} \delta H \,. \tag{4}$$

Considering the outer helical stringer to behave independently for the moment, we expect the counterpart of Eq. (4)

$$\delta R_o = -\frac{H}{16\pi^2 R_o} \delta H \tag{5}$$

to describe the outer stringer. The step width should then change by

$$\delta(R_o - R_i) = \delta R_o - \delta R_i = -\frac{H\delta H}{16\pi^2} \left(\frac{1}{R_o} - \frac{1}{R_i} \right) . \tag{6}$$

The only way to keep the step width constant, corresponding to $\delta(R_o - R_i) = 0$, is to have either zero step width $R_i = R_o$, reducing the double-helix to a single-helix, or to suppress any change in height with $\delta H = 0$. Even though each individual stringer coil can change its height H while keeping its length L constant, the assumed rigid connection between the inner and outer stringers makes the staircase completely rigid.

Next, we relax the constraint that each stringer should maintain its length when the staircase changes its height H. Nevertheless, we will still maintain the assumption of a fixed step width

$$R_o - R_i = const. \tag{7}$$

that translates to $\delta R_i = \delta R_o = \delta R$. The compressible inner stringer helix will still be characterized by its equilibrium length L_i and equilibrium radius R_i. Its deformation caused by changes of its axial height by δH is then described by

$$(L_i + \delta L_i)^2 = (H + \delta H)^2 + (4\pi)^2 (R_i + \delta R_i)^2 \,. \tag{8}$$

Ignoring δL_i^2, δH^2 and δR_i^2 terms in the limit of small deformations, we obtain

$$L_i^2 + 2L_i \delta L_i = H^2 + 2H\delta H + 16\pi^2 (R_i^2 + 2R_i \delta R_i) \,. \tag{9}$$

Subtracting Eq. (1) from Eq. (9), we obtain

$$2L_i \delta L_i = 2H\delta H + 16\pi^2 2R_i \delta R_i \,. \tag{10}$$

With the assumption $\delta R_i = \delta R_o = \delta R$, we can rewrite Eq. (10) and its counterpart for the outer stringer as

$$\begin{aligned} L_i \delta L_i &= H\delta H + 16\pi^2 R_i \delta R \,, \\ L_o \delta L_o &= H\delta H + 16\pi^2 R_o \delta R \,. \end{aligned} \tag{11}$$

Combining all terms containing δR on one side, we can eliminate δR by dividing the two equations. This leads to

$$\frac{L_i \delta L_i - H\delta H}{L_o \delta L_o - H\delta H} = \frac{R_i}{R_o} \tag{12}$$

and, by rearranging terms, to

$$\frac{L_i}{R_i} \delta L_i - \frac{H}{R_i} \delta H = \frac{L_o}{R_o} \delta L_o - \frac{H}{R_o} \delta H = \kappa \,, \tag{13}$$

where κ is a variable to be determined by minimizing the strain energy U of the deformed stringers. U is given by

$$\begin{aligned} U &= \frac{1}{2} C \left(\frac{\delta L_i}{L_i} \right)^2 L_i + \frac{1}{2} C \left(\frac{\delta L_o}{L_o} \right)^2 L_o \\ &= \frac{1}{2} C \left(\frac{\delta L_i^2}{L_i} + \frac{\delta L_o^2}{L_o} \right) , \end{aligned} \tag{14}$$

where C is the force constant describing the elastic response of the stringers to stretching. For a macroscopic stringer with the Young's modulus E and the cross-sectional area A, $C = EA$. From Eq. (13) we get

$$\delta L_i = \frac{H\delta H + \kappa R_i}{L_i} \tag{15}$$

for the inner stringer. Similarly, we get

$$\delta L_o = \frac{H\delta H + \kappa R_o}{L_o} \tag{16}$$

for the outer stringer and can now rewrite the strain energy as

$$U = \frac{1}{2} C \left(\frac{(H\delta H + \kappa R_i)^2}{L_i^3} + \frac{(H\delta H + \kappa R_o)^2}{L_o^3} \right) . \tag{17}$$

The optimum value of κ is obtained from requiring $\partial U / \partial \kappa = 0$. This leads to

$$\frac{(H\delta H + \kappa R_i) R_i}{L_i^3} + \frac{(H\delta H + \kappa R_o) R_o}{L_o^3} = 0 \,, \tag{18}$$

which can be rewritten as

$$(H\delta H + \kappa R_i) R_i L_o^3 + (H\delta H + \kappa R_o) R_o L_i^3 = 0 \,. \tag{19}$$

We can regroup the terms to get

$$H\delta H\left(R_iL_o^3+R_oL_i^3\right)+\kappa\left(R_i^2L_o^3+R_o^2L_i^3\right)=0\,, \quad (20)$$

which yields expressions for the optimum values of κ, δL_i and δL_o. We get

$$\kappa=-H\delta H\frac{R_iL_o^3+R_oL_i^3}{R_i^2L_o^3+R_o^2L_i^3}\,, \quad (21)$$

$$\begin{aligned}\delta L_i&=\frac{H\delta H}{L_i}\left[1-R_i\left(\frac{R_iL_o^3+R_oL_i^3}{R_i^2L_o^3+R_o^2L_i^3}\right)\right]\\&=H\delta H\left[\frac{L_i^2R_o}{R_i^2L_o^3+R_o^2L_i^3}\right](R_o-R_i)\,, \quad (22)\end{aligned}$$

and

$$\begin{aligned}\delta L_o&=\frac{H\delta H}{L_o}\left[1-R_o\left(\frac{R_iL_o^3+R_oL_i^3}{R_i^2L_o^3+R_o^2L_i^3}\right)\right]\\&=H\delta H\left[\frac{L_o^2R_i}{R_i^2L_o^3+R_o^2L_i^3}\right](R_i-R_o)\,. \quad (23)\end{aligned}$$

To interpret this result, let us first consider the inner and outer stringers to be independent first and only then consider the effect of a constant step width separating them. In response to $\delta H>0$, the inner stringer prefers to reduce its radius significantly, but this reduction is limited by the constant-step-width constraint. Thus, the length of the inner stringer is increased and it is in tension. For this to occur, the stairs must have been pulling the inner stringer outwards, and so the steps are subject to tensile stress. In response to increasing its height, also the outer stringer prefers to reduce its radius. But the constant-step-width constraint reduces its radius even more, so that the outer stringer ends up in compression. To accomplish this, the steps must be pulling it inward and again should be subjected to tensile stress. In response to $\delta H<0$, the strains in the inner and the outer stringers will change sign and the steps will be under compressive stress.

The total strain energy amounts to

$$U=\frac{1}{2}C\frac{H^2\delta H^2(R_o-R_i)^2}{R_i^2L_o^3+R_o^2L_i^3}=\frac{1}{2}k\delta H^2\,, \quad (24)$$

where k is the spring constant of the entire double-helix structure, given by

$$k=C\frac{H^2(R_o-R_i)^2}{R_i^2L_o^3+R_o^2L_i^3}\,. \quad (25)$$

We note that in in a single-stringer case, characterized by $R_o-R_i=0$, the axial spring constant k would vanish in our model.

For the initially mentioned spiral staircase in the Loretto chapel, $R_i=0.26$ m, $R_o=1.00$ m, and $H=6.10$ m. From Eq. (1), we get $L_i=6.92$ m and $L_o=13.97$ m.

For the sake of a fair comparison to a straight staircase with a slope given by $\tan(\varphi)$, as seen in Fig. 1(c), we do not use the pitch, but rather the local slope $\tan(\varphi_i)=H/(4\pi R_i)$ of the inner stringer to characterize how steep the staircase is. The Loretto staircase is rather steep near the inner stringer with $\tan(\varphi_i)=1.9$, corresponding to $\varphi_i{\approx}61^\circ$.

The stringers of the Loretto staircase have a rectangular cross-section of 6.4 cm×19.0 cm, and so we have for the cross-section area $A=121$ cm^2. Considering the elastic modulus $E{\approx}10^{10}$ N/m^2 for wood along the grains, we obtain $C=E{\cdot}A=1.2{\times}10^8$ J/m. Thus, the spring constant of the double-helix structure describing the staircase could be as high as $k=4.8{\times}10^6$ N/m.

Now consider the staircase suspended at the top and free to deform in the axial direction. The largest deformation will occur when a load is applied on the lowest step. A person of 100 kg in that location would apply net force $F=981$ N to the staircase, causing an axial elongation of $\delta H=F/k=0.2$ mm, which is very small.

In reality, the staircase is anchored both at the top and the bottom, and its total height is constrained. The weight of a person climbing up the stairs is supported by the fraction x of the staircase below, which is under compression, and the fraction $(1-x)$ of the staircase above, which is under tension. The local axial deflection δh along the staircase is then given by

$$\delta h(x)=\frac{F}{k}x(1-x)\,. \quad (26)$$

The largest deflection occurs in the mid-point of the staircase, with $x(1-x)=1/4$. The local vertical deflection caused by a person of 100 kg standing at this point should be only $\delta h{\approx}0.05$ mm. As expected intuitively, there is no deflection for a person standing either at the top or at the bottom.

III. BENDING DEFORMATION OF A HELICAL COIL

Structurally, the telephone cord in Fig. 1(a), the unsupported helical staircase in Fig. 1(b), and a rubber hose share one important property: all elastic material is on the surface of a hollow cylinder, forming a tube. In a further degree of simplification, we may ignore the interior structure of this elastic tube and describe its stretching, twisting or bending deformations using continuum elasticity theory[7]. So far, we have considered stretching as the dominant response to tensile stress. When a compressive load F is applied to the helical coil, there will always be a reduction in the height H proportional to F/H due to compression. But there will only be bending, which is synonymous with buckling, if FH^2 exceeds a critical value[8,9]. Our task will be to identify this critical value.

This finding agrees with published continuum elasticity results for long-wavelength acoustic phonon modes in

tubular structures[7], which suggest a fundamentally different dispersion relation $\omega_{ZA} \propto k^2$ for bending modes, in stark contrast to $\omega_{LA,TA} \propto k$ for stretching and torsion. Since the vibration frequency is proportional to the deformation energy, it makes sense that bending is preferred to compression at small values of k corresponding to long wavelengths and large H values, and vice versa for short wavelengths and small H values.

As expanded upon further in the Appendix, we consider an elastic tube of radius R and height H that could be either compressed or bent by the displacement amplitude A. We will consider the tube material to be described by the 2D elastic constant c_{11} and the Poisson ratio α. Then according to the equation Eq. (A4) in the Appendix, we obtain for the total axial compression energy

$$U_{c,tot} = \pi c_{11} \left(1-\alpha^2\right) RA^2 \frac{1}{H} \,. \tag{27}$$

Comparing this expression to Eq. (24), we can express c_{11} by

$$c_{11} = k \frac{H}{2\pi R(1-\alpha^2)} \,, \tag{28}$$

where k is given by Eq. (25) and, for the sake of simplicity, we use $R = R_o$.

According to Eq. (1), assuming that load-induced changes of the stringer length L can be neglected, any change in height H would cause a reduction of the radius R and the circumference $2\pi R$. We obtain

$$\begin{aligned} \frac{\delta(2\pi R)}{2\pi R} &= -\frac{H^2}{(4\pi)^2 R^2} \frac{\delta H}{H} = -\frac{(H/R)^2}{16\pi^2} \frac{\delta H}{H} \\ &= -\alpha \frac{\delta H}{H} \,, \end{aligned} \tag{29}$$

thus defining the Poisson ratio

$$\alpha = \frac{(H/R)^2}{16\pi^2} \,. \tag{30}$$

According to Eq. (A9) of the Appendix, the total bending energy is given by

$$U_{b,tot} = 4\pi^5 c_{11} A^2 \left(\frac{R}{H}\right)^3 = 4\pi^4 D_t \frac{A^2}{H^3} \,, \tag{31}$$

where $D_t = \pi c_{11} R^3$ is the flexural rigidity of the tube. The reduction in the height of the tube due to bending is given by

$$\delta H = \int_0^H dx \left[1 + \left(\frac{du_z}{dx}\right)^2\right]^{1/2} - H \approx \frac{2\pi^2 A^2}{H} \tag{32}$$

to lowest order in A, and the work done by the external load is thus

$$F\delta H = \frac{2\pi^2 F A^2}{H} \,. \tag{33}$$

The critical condition for bending to occur is that this work should exceed the total bending energy,

$$F\delta H > U_{b,tot} \,. \tag{34}$$

and translates to

$$FH^2 > 2\pi^2 D_t \,. \tag{35}$$

We can see from the parameters of the Loretto staircase that it is very stable against buckling. From the above equations, we obtain $2\pi^2 D_t = 2\pi^3 c_{11} R^3 = \pi^2 R^2 Hk/(1-\alpha^2)$, which simplifies to $2\pi^2 D_t = \pi^2 R^2 HEA/[H(1-\alpha^2)] = \pi^2 R^2 EA/(1-\alpha^2)$. Since $R \approx R_o = 1$ m, $\alpha = 0.24$, and $EA = 1.2\times10^8$ J/m, we get $2\pi^2 D_t = 1.25\times10^9$ Jm. Assuming a compressive load $F = 10^3$ N, this quantity is vastly greater than $FH^2 = 10^3 \times 6.1^2 = 3.7\times10^4$ Jm. The load would have to be increased by more than four orders of magnitude, or the height increased by more than two orders of magnitude, to cause buckling.

IV. ELASTIC BEHAVIOR OF SIMILAR HELICAL STRUCTURES IN NATURE

Every helical structure, from the coiled telephone cord in Fig. 1(a) to the spiral staircase in Fig. 1(b) and to submicron-sized α-helices found in proteins, can be mapped topologically onto a helical coil. The helix we describe here, which turns out very rigid, consists of two helical coils with different radii, separated by a constant distance. This particular design could clearly be utilized to form man-made nanostructures that will be very rigid.

It is tempting to explore whether any existing structures in Nature may look similarly and behave in a similar manner. Among the biomolecules that immediately come to mind is the double-stranded DNA that, coincidentally, is also left-handed. DNA, however, does not fulfill the constant-step-width assumption, since the bases from the two strands are non-covalently bound in pairs, forming a "breathing" rather than a rigid unit. Another system known for its toughness, collagen[10], has only some inter-strand covalent bonding, but not at every step. Moreover, its tripe-helix structure differs from the model we discuss. After a long search, we believe there are no real counterparts in Nature of the structure we describe, at least not among biomolecules.

V. DISCUSSION

Our main objective was to elucidate the origin of the previously unexplained high rigidity of the unsupported spiral Loretto staircase by developing a suitable formalism. Our numerical results should be taken as rough estimates. We expect the local axial deflections δh of this staircase caused by load to be significantly larger than the estimated values presented above. The estimated value of the effective spring constant of the staircase helix is

likely to be reduced significantly by defects and human-made joints in this all-wooden structure. Further reduction would come from considering other deformation modes including lateral compression or stretching of the wooden steps and, to some degree, bending. Elastic response to shear stress in the stringers should significantly contribute to the spring constant especially in low-pitch spirals, with the coiled telephone cord as an intuitive example. Even though the spiral staircase of Fig. 1(b) is a high-pitch spiral, allowing for shear deformations in the stringers should further reduce its effective force constant. Even if all these factors combined should decrease the force constant by 1-2 orders of magnitude, we may still expect a maximum local axial deflection δh of not more than $1-2$ cm in case that each of the 33 steps were loaded by the weight of a person. As expanded above, since the height is significantly larger than the radius, bending should not play a significant role as a possible response to applied load. We also note that at a later stage, the staircase had been augmented by a railing, shown in Fig. A1(a) in the Appendix. This railing does not affect the elastic response of the staircase under load.

As mentioned above, we have not found any asymmetric double-helix structure in Nature that is rigid and does not stretch much. Should such a structure exist, its stiffness should benefit from a constant separation between the helical coils.

VI. SUMMARY AND CONCLUSIONS

In summary, we have used continuum elasticity theory to describe the elastic behavior of helical coils with an asymmetric double-helix structure and have identified conditions, under which they become very rigid. Theoretical insight gained for macro-structures including a stretched telephone cord and an unsupported helical staircase is universal and of interest for the elastic behavior of helical structures on the micro- and nanometer scale.

ACKNOWLEDGMENTS

A.G.E. acknowledges financial support by the South African National Research Foundation Grant No. 80798. D.T. acknowledge financial support by the NSF/AFOSR EFRI 2-DARE grant number EFMA-1433459 and the hospitality of the University of the Witwatersrand, South Africa, where this research was performed. We thank Garrett B. King for his assistance with the literature search for rigid helical structures in Nature and their schematic graphical representation and thank Dan Liu for useful discussions.

APPENDIX

A. Deformation Energy due to Compression and Bending

As introduced in the main text, any helical structure may be mapped onto an elastic tube of radius R and height H that could be either compressed axially or bent. We will consider the tube aligned along the x-direction and the tube material to be described by the 2D elastic constant[7] c_{11} and the Poisson ratio α. We will consider the local distortions to be described by

$$u_x = (-A)\frac{x}{H} \tag{A1}$$

in the case of axial compression, and

$$u_z = A\left[\sin\left(2\pi\frac{x}{H} - \frac{\pi}{2}\right) + 1\right] \tag{A2}$$

in the case of bending, where A denotes the amplitude of the distortion.

According to Eq. (A2) of Reference [7], the compression energy per length is given by

$$\begin{aligned} U_c &= \frac{1}{2} 2\pi R c_{11}\left(1-\alpha^2\right)\left(\frac{du_x}{dx}\right)^2 \\ &= \pi c_{11}\left(1-\alpha^2\right) R\left(\frac{A}{H}\right)^2 . \end{aligned} \tag{A3}$$

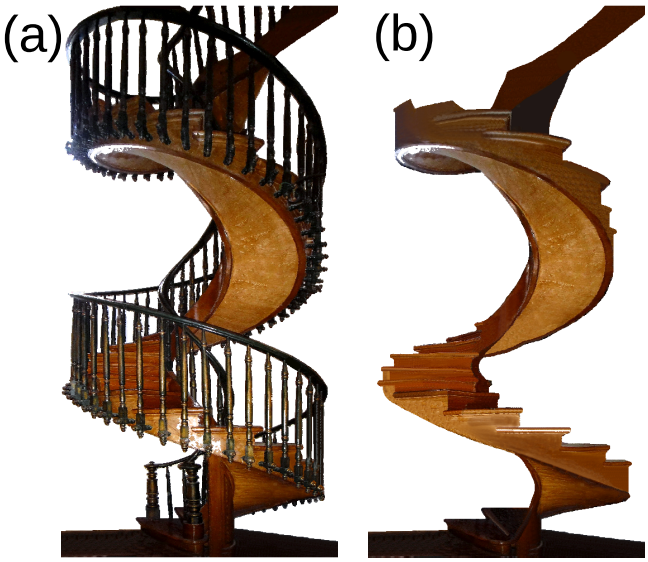

FIG. A1. Retouched photographs, with the background digitally removed, of the spiral staircase in the Loretto Chapel, Santa Fe, New Mexico. (a) Current view of the staircase including the railing, which had been added long after construction. (b) Likely view of the staircase as constructed, with no railing.

The total compression energy of the tube of height H is then

$$U_{c,tot} = U_c H = \pi c_{11} \left(1 - \alpha^2\right) R A^2 \frac{1}{H} \,. \tag{A4}$$

According to Eq. (A15) of Reference [7], the bending energy per length is given by

$$U_b = \frac{1}{2}(\pi c_{11} R^3 + \pi D R) \left(\frac{d^2 u_z}{dx^2}\right)^2 \,. \tag{A5}$$

Since the flexural rigidity D of the wall "material" vanishes due to the separation between adjacent helix strands, we obtain

$$U_b = \frac{1}{2}\pi c_{11} R^3 \left(\frac{d^2 u_z}{dx^2}\right)^2 \,. \tag{A6}$$

Using the expression in Eq. (A2) for the bending deformation, we obtain

$$\left(\frac{d^2 u_z}{dx^2}\right)^2 = A^2 \left(\frac{2\pi}{H}\right)^4 \sin^2\left(2\pi \frac{x}{H} - \frac{\pi}{2}\right), \tag{A7}$$

which leads to

$$U_b = \frac{1}{2}\pi c_{11} R^3 A^2 \left(\frac{2\pi}{H}\right)^4 \sin^2\left(2\pi \frac{x}{H} - \frac{\pi}{2}\right). \tag{A8}$$

The total bending energy is obtained by integrating U_b in Eq. (A8) along the entire height H of the bent tube, yielding

$$U_{b,tot} = 4\pi^5 c_{11} A^2 \left(\frac{R}{H}\right)^3 \,. \tag{A9}$$

Finally, assuming the same distortion amplitude A for bending and compression, we can determine the ratio of the compression and the bending energy

$$\frac{U_{c,tot}}{U_{b,tot}} = \frac{1 - \alpha^2}{4\pi^4} \left(\frac{H}{R}\right)^2 \tag{A10}$$

that is independent of the amplitude A and the elastic constant c_{11}. We see that for $H >> R$, $U_{c,tot} >> U_{b,tot}$, indicating that bending is energetically more affordable and thus dominates. The opposite situation occurs for $H << R$, when axial compression dominates.

B. Photographs of the Staircase

Retouched photographs of the spiral staircase in the Loretto Chapel, Santa Fe, New Mexico, are presented in Fig. A1.

* tomanek@pa.msu.edu

[1] Bill Brokaw, *Loretto Chapel: The Miraculous Staircase* (The Creative Company, Lawrenceburg, Indiana, USA, 2002).

[2] A. E. H. Love, *A Treatise on the Mathematical Theory of Elasticity* (Cambridge University Press, Cambridge, UK, 1927).

[3] D Fakhreddine, T Mohamed, A Said, D Abderrazek, and H Mohamed, "Finite element method for the stress analysis of isotropic cylindrical helical spring," Europ. J. Mech. A-Solids **24**, 1068–1078 (2005).

[4] L. M. Zubov, "The problem of the equilibrium of a helical spring in the non-linear three-dimensional theory of elasticity," J. Appl. Math. Mech. **71**, 519–526 (2007).

[5] D. Tomanek, W. Zhong, and E. Krastev, "Stability of multishell fullerenes," Phys. Rev. B **48**, 15461–15464 (1993).

[6] Dan Liu, Arthur G. Every, and David Tománek, "Continuum approach for long-wavelength acoustic phonons in quasi-two-dimensional structures," Phys. Rev. B **94**, 165432 (2016).

[7] Dan Liu, Arthur G. Every, and David Tománek, "Long-wavelength deformations and vibrational modes in empty and liquid-filled microtubules and nanotubes: A theoretical study," Phys. Rev. B **95**, 205407 (2017).

[8] Leonhard Euler, *De curvis elasticis*, Methodus inveniendi lineas curvas maximi minimive proprietate gaudentes (Lausanne and Geneva, Switzerland, 1744).

[9] Stephen P. Timoshenko and James M. Gere, *Theory of Elastic Stability*, 2nd ed. (McGraw-Hill, New York, 1961).

[10] Rita Berisio, Luigi Vitagliano, Lelio Mazzarella, and Adriana Zagari, "Crystal structure of the collagen triple helix model $[(\text{Pro-Pro-Gly})_{10}]_3$," Protein Sci. **11**, 262–270 (2002).